Pergamon

Journal of Structural Geology, Vol. 19, No. 12, pp. 1461 to 1477, 1997

0191-8141/97 $17.00 + 0.00

PII: S0191-8141(97)00056-4

Nucleation and growth of strike-slip faults in limestones from Somerset, U.K.

EMANUEL J. M. WILLEMSE*

Rock Fracture Project, Department of Geological and Environmental Sciences, Stanford University, Stanford, CA 94305-2115, U.S.A.

DAVID C. P. PEACOCK

Rock Deformation Research Group, Department of Earth Sciences, University of Leeds, Leeds LS2 9JT, U.K.

and

ATILLA AYDIN

Rock Fracture Project, Department of Geological and Environmental Sciences, Stanford University, Stanford, CA 94305-2115, U.S.A.

(*Received* 23 *May* 1997; *accepted in revised form* 22 *July* 1997)

Abstract—Small-scale structures along strike-slip fault zones in limestones exposed around the Bristol Channel, U.K., suggest that pressure solution plays a key role during fault nucleation and growth. Incipient shear zones consist of en échelon veins. The first generation of solution seams form due to bending of the intact rock (bridge) between overlapping veins. As the bridge rotates, slip occurs along the seams, linking the veins, causing cm-scale calcite-filled pull-apart structures to form and allowing fault displacement to increase. A second generation of solution seams forms at the tip of the sliding seams. As displacement increases further, causing larger rotation, slip also can occur along these second-generation solution seams, producing the third generation of solution seams as well as tail cracks (pinnate veins) at their tips. These three generations of solution seams all contribute to the formation of individual fault segments. Fourth and fifth generations of solution seams occur within larger-scale contractional oversteps between side-stepping fault segments. The oversteps are breached by slip along these localized solution seams, eventually leading to the formation of a distinct through-going fault with several metres of displacement.

The initial en échelon veins, solution seams of various generations and tail cracks progressively fragment the fault-zone material as fault slip accumulates. Slip planes nucleate on these pre-existing discontinuities, principally along the clay-enriched, weaker solution seams. This can be observed at a variety of scales and suggests that Mode II shear fracturing does not occur as a primary fracture mechanism, but only as a macroscopic phenomenon following Mode I (veins and tail cracks) and anti-mode I (solution seams) deformation. It appears that solution seams can play a similar role to microcracks in localizing a through-going slip plane. This micromechanical model of faulting may be applicable to some other faults and shear zones in host rocks which are prone to pressure solution. © 1997 Elsevier Science Ltd.

INTRODUCTION

Shear failure leading to the formation of faults in rock is not well understood. The process of faulting is rather complex and, once formed, faults obliterate the evidence of the initial stages as displacement accumulates. The current understanding of the mechanics of shear failure is based primarily on experimental data, augmented with a few field studies (e.g. Martel *et al.*, 1988). One important outcome of these studies is that shear failure is a localization phenomenon (Rudnicki and Rice, 1975) that does not adhere to a single model, but rather may involve a variety of mechanisms.

In porous granular materials, grain comminution, pore collapse and cataclasis play important roles (Mandl *et al.*, 1977; Menendez *et al.*, 1996). In sand-box experiments with unconsolidated sand, shear bands form by rolling and sliding of intact grains (Horsfield, 1977; Franssen *et al.*, 1994). In poorly lithified pelitic rocks, elongate clay minerals within a narrow zone rotate into an orientation parallel to the direction of slip (Maltman, 1987, 1994). Experiments on low-porosity granites and lithified sandstones indicate that opening-mode microcracking plays an important role in the initial stages of shear failure (Brace and Bombolakis, 1963; Brace *et al.*, 1966; Scholz, 1968; Petit and Barquins, 1988; Zhao *et al.*, 1993; Moore and Lockner, 1995).

A few field studies have been undertaken to describe incipient faults and to determine how such faults nucleate and grow. Many of the mechanisms operating in the laboratory can also be recognized in the field (Friedman, 1969; Engelder, 1974; Aydin, 1978; Aydin and Johnson, 1978; Knipe and White, 1979; Kanaori *et al.*, 1991; Antonellini *et al.*, 1994). Field studies also expand

*Present address: EPT-SG, Research and Technical Services, Shell International Exploration and Production, Volmerlaan 8, 2288GD Rijswijk, The Netherlands.

experimental work: some mechanisms observed in outcrops have not been reproduced in the laboratory, perhaps because of the materials used (clay, sand, quartzite and granite), the limited sample size or the applied boundary conditions (strain rate, confining pressure, temperature, etc.). For example, some larger-scale faults, tens to hundreds of metres long, appear to nucleate along pre-existing joints and grow by subsequent linkage of such sheared joints along mode I tail cracks, also called wing cracks, splay cracks and pinnate veins (Segall and Pollard, 1983; Hancock, 1985; Hancock and Barka, 1987; Martel *et al.*, 1988; Engelder, 1989; Cruikshank *et al.*, 1991).

The purpose of this paper is to describe the nucleation and growth of strike-slip faults in limestones exposed along the Bristol Channel, U.K., and to illustrate that pressure solution can play an important role in the micromechanics of faulting. After a general description of the regional geological setting and the mapping methods employed, the various types of fault-zone structures and their spatial relationships are documented. Based on this, on the fault-zone architecture and its hierarchical evolution, and on rock mechanical arguments, we propose a model for the development of strike-slip faults zones in limestones. We compare these results with previous work and conclude that this model may be appropriate for other rock types. Finally, we comment upon the intimate relationship between deformation mechanisms, rock properties (e.g. rheology, solubility) and some boundary conditions (e.g. loading rate, temperature) that accompany faulting.

REGIONAL GEOLOGY AND MAPPING TECHNIQUES

The strike-slip faults are exposed on sub-horizontal bedding planes of Lower Jurassic limestones between East Quantoxhead (grid reference ST122439) and Lilstock (ST196462), Somerset, U.K. (Fig. 1). The mean thickness of the limestone beds is about 0.2 m, while mudrocks between the limestones are about 0.5 m thick (Whittaker, 1983; Peacock and Zhang, 1994). The area is part of the Bristol Channel Basin, which underwent N–S extension during the Mesozoic (Chadwick, 1986; Brooks *et al.*, 1988; Donato, 1988) producing E–W-striking normal faults and calcite-filled veins (Peacock, 1991; Peacock and Sanderson, 1991; Bowyer and Kelly, 1995). Late Cretaceous or early Tertiary N–S shortening led to development of the strike-slip faults described below. The N–S contraction also caused E–W-striking thrusts and reverse reactivation of the E–W-striking normal faults (McLachlan, 1986; Peacock and Sanderson, 1992; Bowyer and Kelly, 1995). During this phase, N–S-striking, sub-vertical calcite-filled veins formed locally in the close vicinity of the strike-slip, thrust and reverse

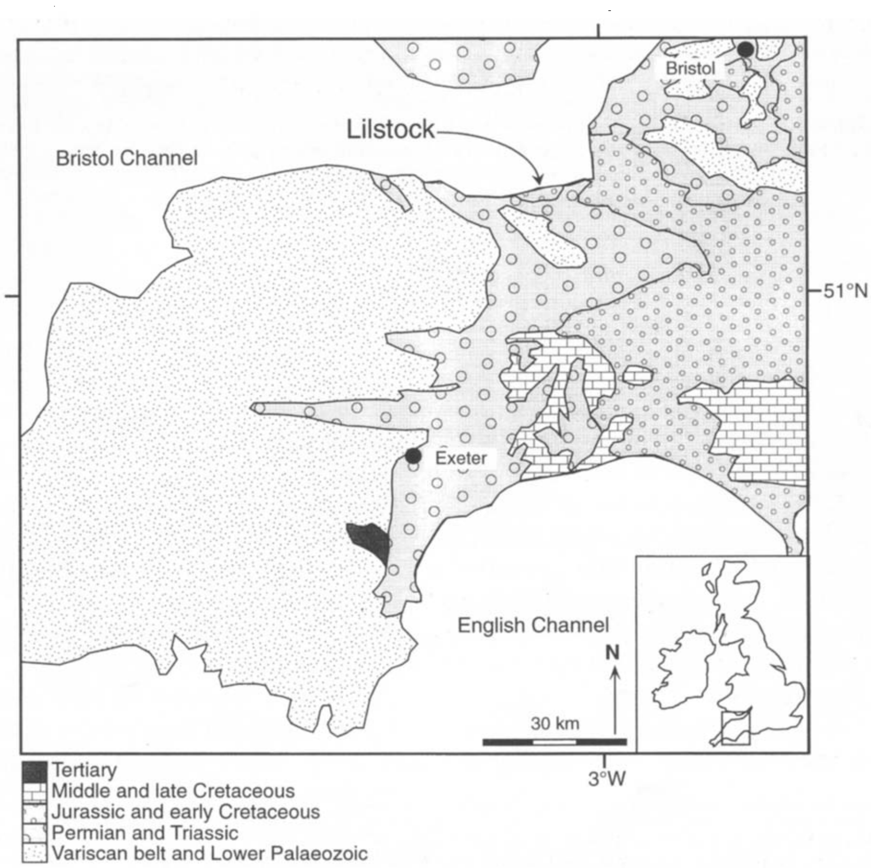

Fig. 1. Location map showing simplified surface geology (after Chadwick, 1986).

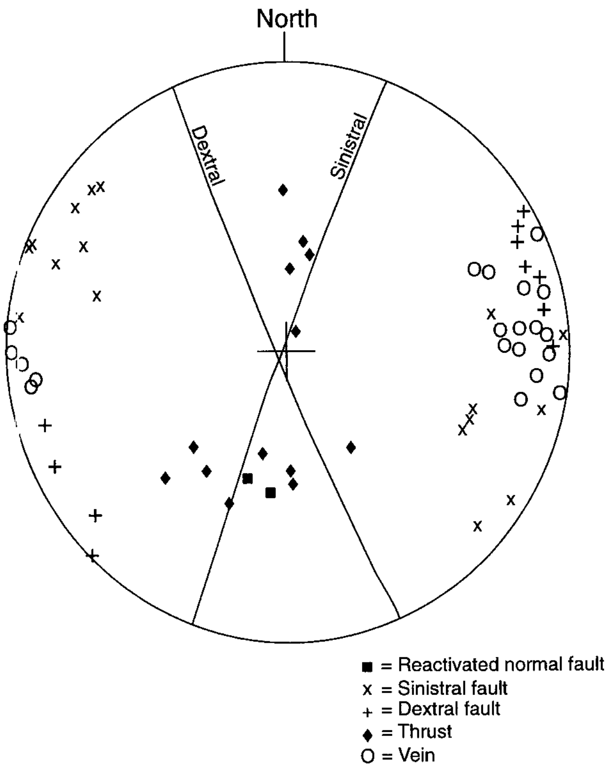

Fig. 2. Equal-area projection of poles to contractional faults and veins at Kilve, Somerset, related to the N–S contractional event. The mean great circles for the conjugate strike-slip faults, and the inferred orientations of the principal stress axes, are shown. The related solution seams are sub-vertical and strike E–W ± 20°, but are difficult to measure (see Peacock and Sanderson, 1992, fig. 7).

reactivated normal faults (Bowyer and Kelly, 1995). The orientations of these structures are illustrated in Fig. 2.

In the study area dextral and sinistral strike-slip faults occur, conjugate about the N–S contraction direction (Fig. 2). These faults have maximum displacements of more than 2 m and can be a few hundred metres long (Peacock and Sanderson, 1995b). Each fault consists of several side-stepping segments that are several tens of metres long. Variation in pull-apart widths suggests that the slip distribution is similar to that measured along other faults (Fig. 3): slip is greatest in the middle part of the fault zone and decreases approximately linearly to zero at the fault tip (Peacock and Sanderson, 1995a). Slickenside lineations are often slightly oblique to bedding, with minor vertical separation of bedding planes occurring (Peacock and Sanderson, 1995b). Bedding planes may be locally rotated in relay ramps between adjacent fault segments. Peacock and Sanderson (1995b) describe the geometry of these m-scale relay ramps and discuss linkage of adjacent segments. In this contribution, however, we focus on the development of individual fault segments, and as such we address earlier stages of fault development in which slip is at most a few hundred millimetres. The examples described are from strike-slip faults with displacements of up to several metres, an example of which is illustrated in Fig. 3. Relicts of these incipient fault structures are poorly preserved in the walls of larger-displacement faults.

Along each fault segment there exists a variety of elementary structures such as veins, pull-aparts, solution seams and slip planes. The fault zones were mapped at a scale of 1:1 by tracing the various types of structures onto sheets of acetate which were taped to the bedding planes. This method is quick and accurate, except for veins which are < 0.5 mm wide because the pens used produce lines are about 0.5 mm wide. The length of mapped structures varies from a few centimetres to about 1 m. Fault displacements were determined by measuring the widths of pull-aparts in the direction parallel to the slip surfaces with a vernier calliper (Peacock and Sanderson, 1995a).

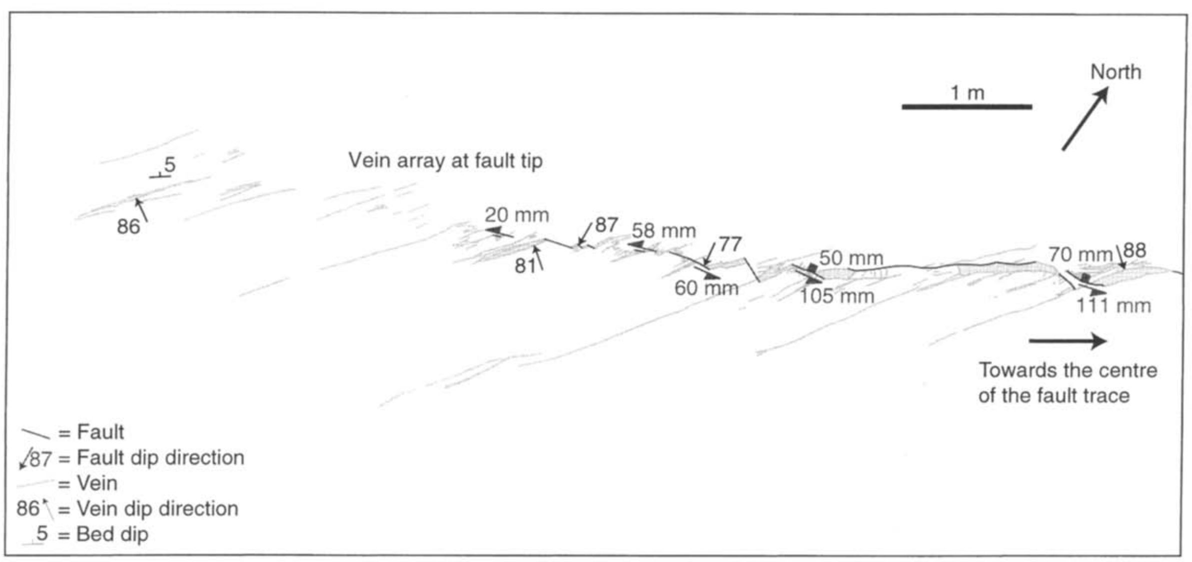

Fig. 3. Map of a strike-slip fault near Lilstock which dies out into a series of pull-aparts, with en échelon veins beyond the fault tip. This fault is an E–W-striking normal fault which was reactivated as a sinistral strike-slip fault (Peacock *et al.*, in preparation). Vertical and horizontal separations are shown.

OBSERVED FAULT-ZONE STRUCTURES

The structures observed comprise several generations of veins and pressure-solution seams. Structures with the simplest geometries occur ahead of the fault tip. These structures capture the incipient stage of shearing because there is little or no demonstrable shear displacement across the zone. Several metres to decimetres ahead of a strike-slip fault zone, there commonly exists an array of veins sub-parallel to the fault (Figs 3 & 4a). The veins are approximately perpendicular to bedding planes (Fig. 2) and are arranged en échelon, with the angle between the average orientation of the array and individual veins varying from a few degrees to about 45° (Figs 3 & 4). Some veins are sigmoidal, but most are straight. The vein length varies from 10 mm to over 1 m. The maximum vein width is typically from 1 to several mm. The width is approximately constant along most of the trace of a vein, but decreases rapidly in the vicinity of neighbouring veins (Fig. 4a & b). Adjacent veins most commonly overlap. In some cases, the overlap between veins is much greater than their spacing. Such overlapping portions of a vein are generally very slender, forming a tail-like prolongation of the much wider main vein. Although en échelon

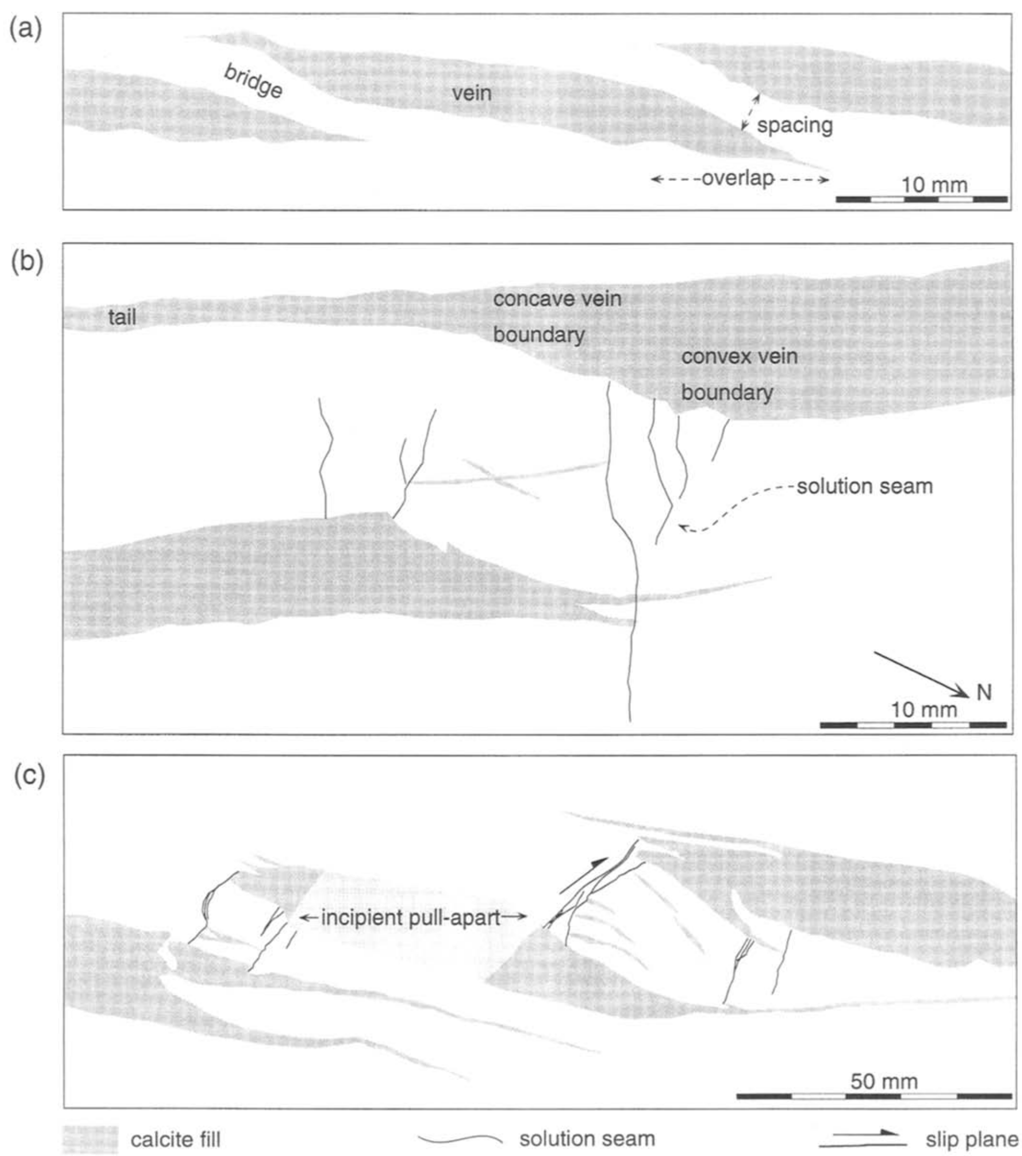

Fig. 4. En échelon veins. The map in Fig. 3 illustrates the relationship between (a), (b) and (c) at a fault tip. (a) Centimetre-scale calcite-filled veins. The vein width is approximately constant along most of the central vein, but decreases rapidly in the regions of overlap with the neighbouring veins (Peacock, 1991). (b) Close-up of a bridge between two overlapping veins. Solution seams (thin black lines) emanate from the convex-outward side of the veins, where bending of the bridge material leads to contraction. Note two minor cemented veins (grey) crossing each other in the centre of the bridge. (c) Thick en échelon veins with thin, tail-like prolongations where overlapping with neighbouring veins. The bridges between neighbouring veins are characterized by two symmetrically arranged zones of solution seams, and occasionally by one or more calcite veins. The central vein in the array may represent the incipient stages of a pull-apart structure (lighter grey shading). From a loose boulder.

vein patterns are often regarded as shear-strain indicators (e.g. McCoss, 1986), there is no measurable shear displacement across the vein arrays in this stage.

Closer to the fault, pressure-solution seams (also called stylolites) appear in the bridges between veins (Fig. 4b & c). The dark, braiding solution seams only occur within the region of vein overlaps (bridges). They are preferentially located on the convex-outward side of each boundary vein (see 'solution seam' in Fig. 4b). Most bridges are characterized by two symmetrically arranged zones of solution seams, but generally only one zone is well developed. Incipient solution seams terminate within the bridge (Fig. 4b), but well-developed solution seams extend from one vein to the other (Fig. 4c) or occasionally cross the adjacent vein, forming a dark trace through white calcite crystals. Such intersections or crossings do not occur at the concave-inward side of a vein, but more towards the vein tip.

Pull-aparts occur further away from the fault tips, representing the first clear indication of shear displacement along the fault zone (Fig. 5). The initial shearing is accommodated by slip across the solution seams within the bridges. The amount of shear displacement accommodated by the pull-aparts is up to several tens of millimetres. The widths of pull-aparts increase towards the centre of a fault zone and decrease toward the tips (e.g. Fig. 3). The gradual progression towards the centre of the fault zone from en échelon veins to incipient pull-aparts is illustrated in Fig. 5(d).

A pull-apart, and therefore a distinct fault, forms when slip occurs on the solution seams that link a vein with adjacent vein segments. Opening occurs only along the central part of the vein, in-between the slipping solution seams (Fig. 5). The remaining outer parts of the vein do not experience significant further opening and commonly form distinct 'tails' at two diagonally opposing corners of the pull-apart (Fig. 5a–c). In many cases, only one tail is observed. The slip surfaces that bound incipient pull-aparts occur within braided networks of dark solution seams. An example is the middle vein in Fig. 4(c) which appears in its central part to have widened a few millimetres due to incipient pull-apart (lighter grey shading). For another example of incipient pull-apart, see Peacock and Sanderson (1995b, fig. 4a). With increased displacement across the fault zone, slip is concentrated along a single or a few dark seams (Fig. 5a-c), which in thin section reveal concentrations of clay material (Peacock and Sanderson, 1995a). The angle between the slip surfaces and the original veins, which are postulated to be parallel to the opening sides of the pull-aparts or the tails extending from them, can be up to 90°. Pull-aparts show a wide range of geometries, described in more detail by Peacock and Sanderson (1995b). These are distinct from sigmoidal veins (e.g. Ramsay and Huber, 1987), which typically have more rounded edges and which are not linked by distinct fractures.

Further away, at about 0.5 m from the tip of the fault zone, displacement increases to the centimetre range (Figs 3 & 6). The structure along this part of the fault zone is more complex. Pull-aparts grow wider, and may overlap and link, forming a fault zone filled by calcite. In the example shown in Fig. 6, displacements along the fault increase from zero in the tip region to about 60 mm in the south. As the slip increases, the pull-aparts merge, forming a composite pull-apart with continuous calcite fill. Within the light-coloured calcite cement, individual pull-aparts can often be distinguished based on the darker colour of the slipped solutions seams. Although some 'tails' are present, most have been sheared off the associated pull-apart.

Pressure-solution seams are abundant in the vicinity of the fault zone shown in Fig. 6. These seams represent the second generation of solution seams, the density of which is greater on the western side of the fault zone (contractional quadrant) compared to the eastern side (extensional quadrant, see also the inset to Fig. 6). The seams are relatively evenly spaced at some distance from the fault, but are weakly clustered near the fault zone. Such clusters of solution seams are located at, and appear to radiate outwards from, pull-apart corners where slip planes die out (marked by asterisks in Fig. 6). These solution seams apparently have also formed in the contractional quadrant of the short slip planes (see the inset to Fig. 6). The angle between the slip planes and solution seams at their termination is generally about 70°. Very narrow opening-mode veinlets may occur next to, and parallel to, the opening sides of pull-aparts (diamonds in Fig. 6). Most veinlets become wider towards the slip plane and occur on the side opposite the clustered solution seams, i.e. in the extensional quadrant of the slip planes (see also the inset to Fig. 6).

There is evidence that some of the second-generation solution seams clustered in the immediate vicinity of the fault segments experience slip with increasing deformation. In outcrop, these sheared solution seams often are preferentially weathered, forming a series of short, parallel grooves at a high angle to the fault zone (Fig. 7a & b). Slip along these second-generation solution seams is evident from the third generation of solution seams and tail cracks that develop in the opposite quadrants at the tips of the sheared seams. The strike orientation of the tail cracks is generally within approximately 30° of the early stage en échelon veins. Slip along the second-generation solution seams is antithetic to that of the fault zone, in agreement with the expected sense of rotation. When densely spaced, high-angle slip planes can form a bookshelf-type arrangement. In such cases, tail cracks and third-generation solution seams may link up, forming a through-going, jagged surface that is approximately parallel to the local trend of the fault zone. An incipient stage example of such a jagged surface, which is not yet fully continuous, is visible in the lower left of Fig. 7(b).

At this stage, the total displacement across the fault zone is several tens of millimetres. An irregular continuous fault zone has developed with a complex arrange-

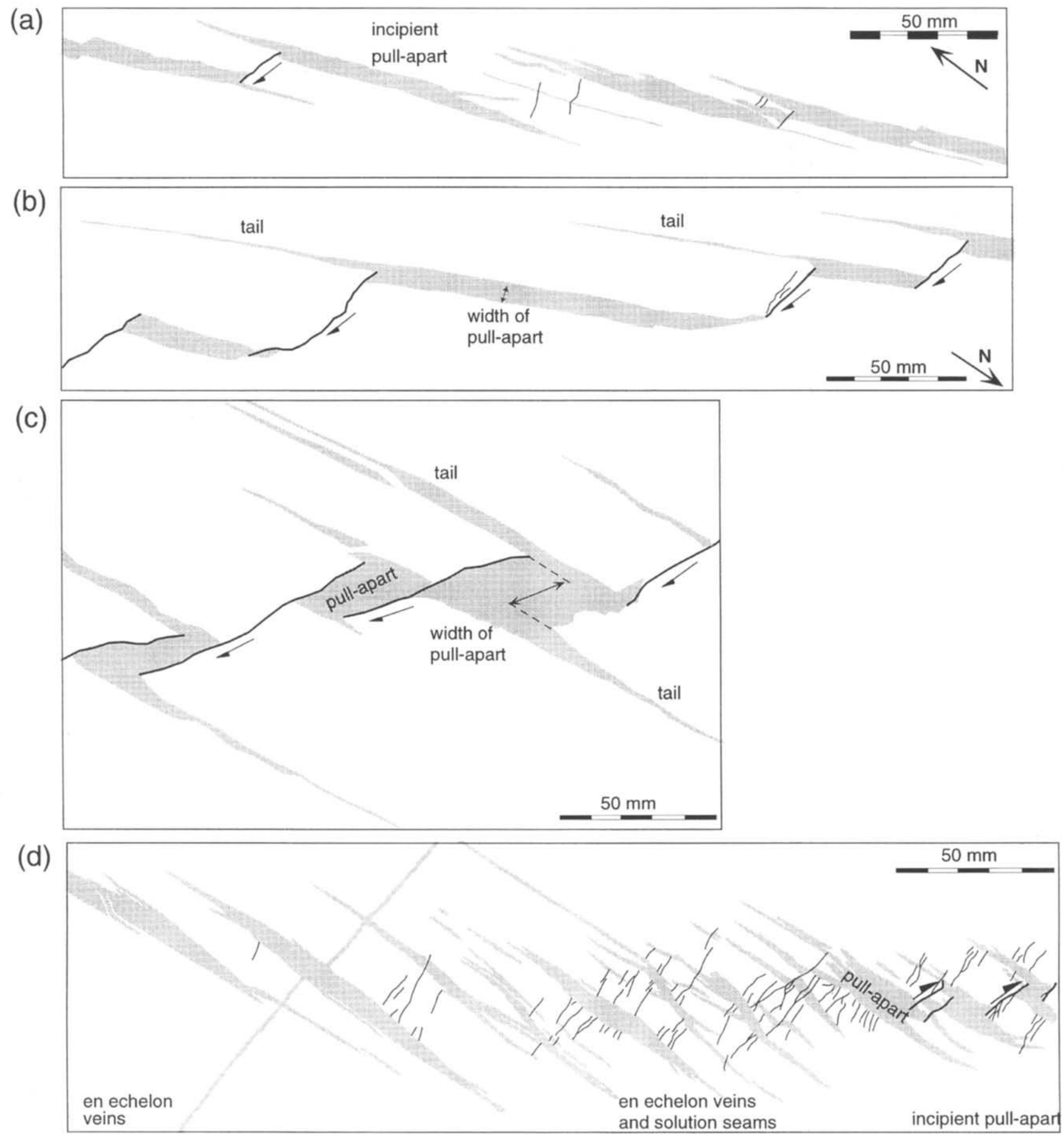

Fig. 5. Stages in the development of pull-aparts. (a) A vein array with incipient pull-aparts on the left and right. Slip planes are indicated by thick black lines. The central bridge is cut by solution seams without demonstrable shear. (b) Intermediate-stage pull-aparts with tails. Slip planes connecting pull-aparts are associated with solution seams and can be wavy (left of centre) or straight (right of centre). (c) Well-developed pull-aparts with characteristic tail structures at opposing corners. Displacement along the slip planes is sufficient to link some pull-aparts. From a loose boulder. (d) Spatial relationship between en échelon veins (left side), en échelon veins and solution seams (centre), and incipient pull-aparts (right side). Note the increasing density of solution seams towards the right. From a loose boulder. Note: (a) and (d) are mirror images of the exposures to allow comparison with Fig. 4(b & c).

ment of vein material, slip planes and solution seams. Although the fault zone commonly has a near-breccia appearance, the various types of structures, and their interrelationships and hierarchy, generally remain recognizable. Further along the strike of the fault, slip across the fault zone may eventually decrease as the other tip of the fault segment is approached. Some fault segments die out into en échelon veins or into an array of tail cracks (called pinnate veins or horsetail structures by Hancock, 1985; Hancock and Barka, 1987; Engelder, 1989; Peacock and Sanderson, 1995b). More commonly, however, slip is transferred to the neighbouring fault segment

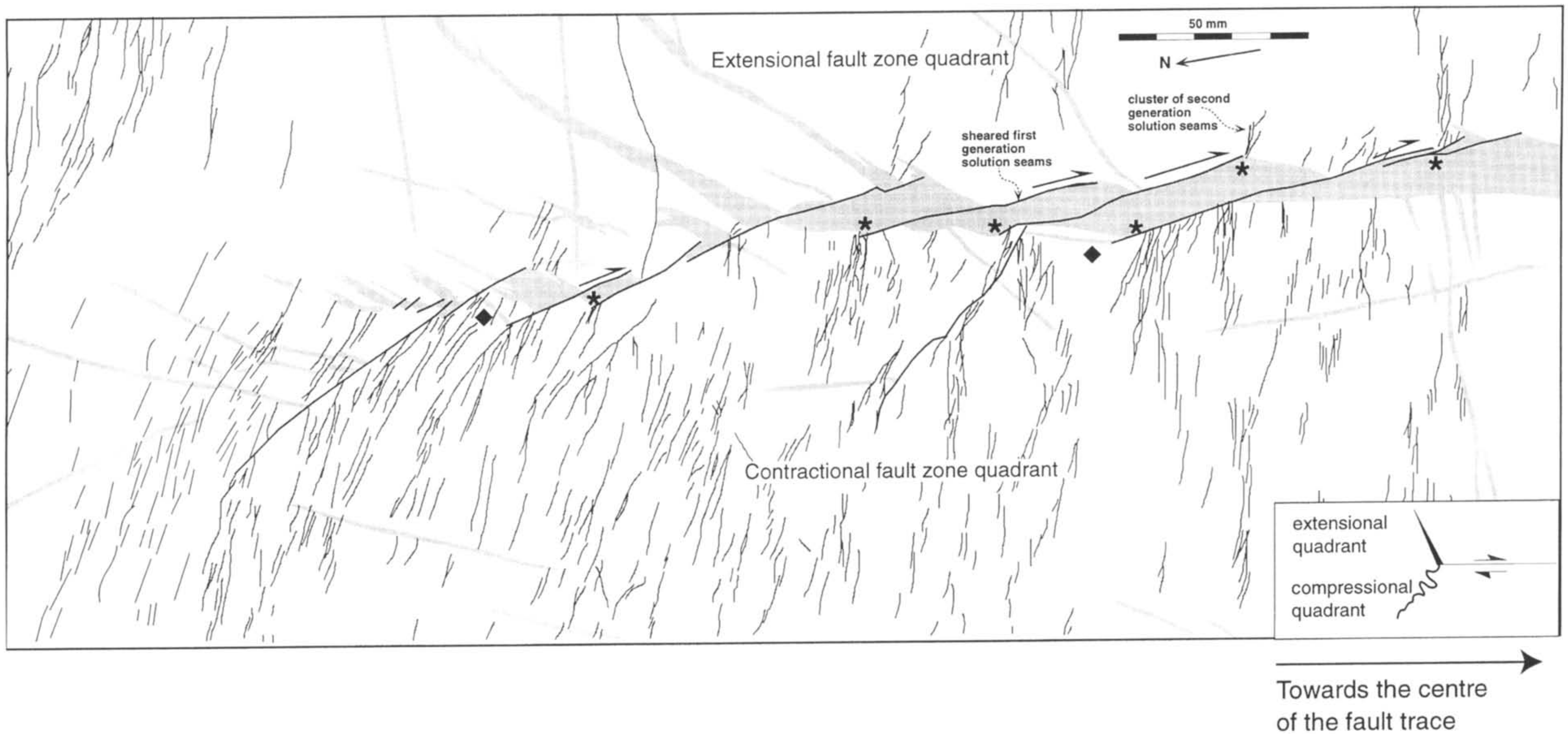

Fig. 6. The termination of a strike-slip fault zone, with the centre of the fault trace occurring to the south of the mapped area. Most solution seams occur to the west of the fault, in the contractional quadrant. Close to the fault zone, the second-generation solution seams are clustered at the corners of pull-aparts where slip planes terminate (marked by asterisks). Diamonds indicate veinlets associated with pull-aparts. Inset shows the distribution of extensional and contractional quadrants about the termination of a strike-slip fault. The occurrence of solution seams in the contractional quadrants can be observed both at the scale of the entire mapped fault zone and at the scale of the smaller slip planes (asterisks).

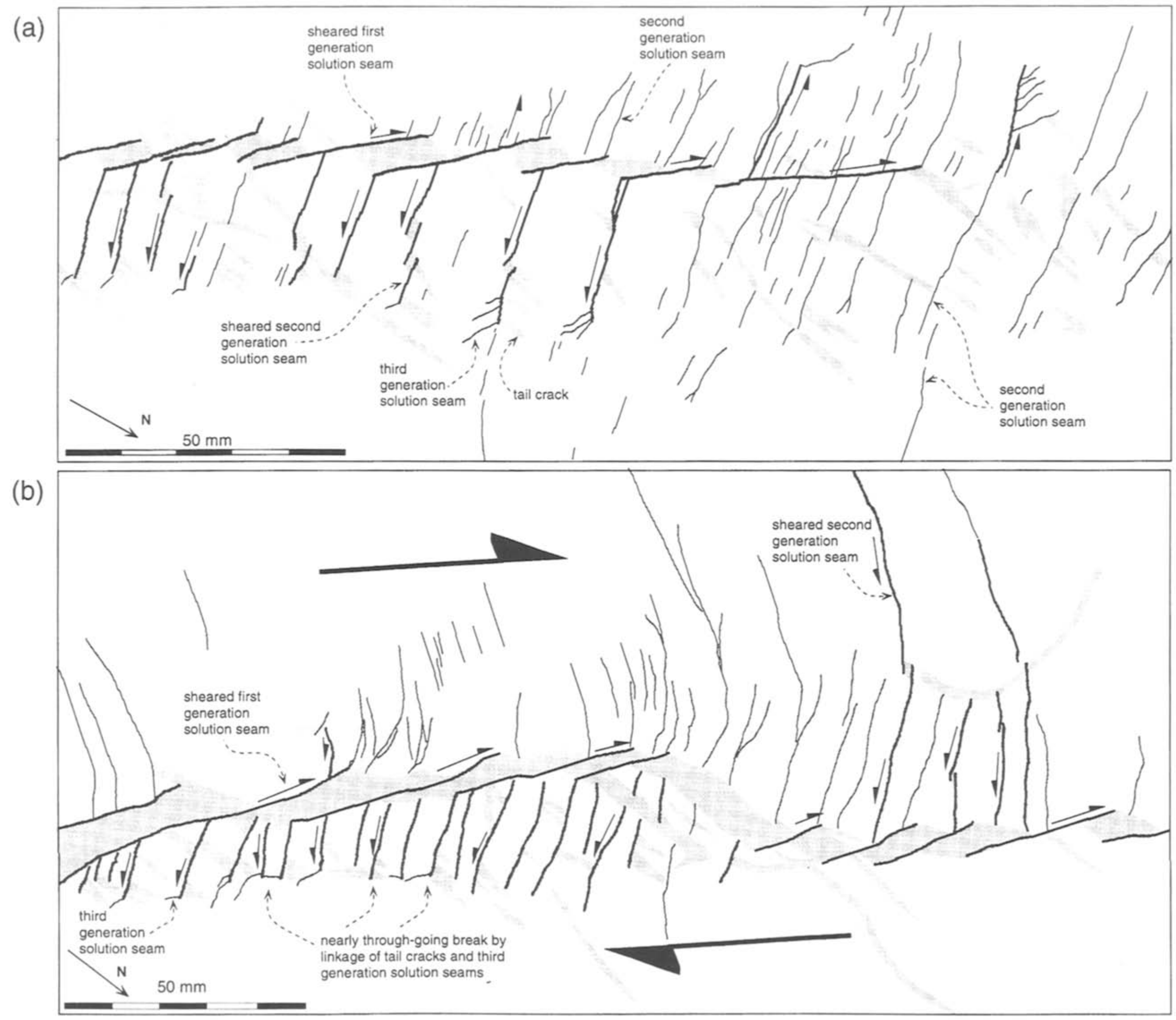

Fig. 7. Well-developed fault zones. (a) Sheared second-generation solution seams are orientated at a high angle to the fault zone. Slip along the second-generation solution seams is antithetic to the main fault zone, as indicated by the tail cracks and third-generation solution seams at their tips. (b) A series of densely spaced second-generation solution seams. Blocks between some seams appear to have rotated clockwise, causing antithetic shear. The sheared seams below the main fault are so closely spaced that the tail cracks and third-generation solution seams at the tip of neighbouring sheared seams may intersect, forming a nearly through-going, jagged discontinuity parallel to the fault zone. The drawings in (a) and (b) are mirror images of the exposure to facilitate comparison to other figures.

across a relay zone via another complex assemblage of structures.

In the study area, deformation in m-scale relay zones between neighbouring fault segments involves formation of veins, solution seams, and syn- and antithetic faults (Peacock and Sanderson, 1995b). Adjacent side-stepping segments form contractional relay ramps. Pressure-solution seams form preferentially within the contractional relay ramps, and are orientated oblique to the adjacent fault segments (Fig. 8). We refer to these solution seams as the fourth generation. Although no cross-cutting relationships can be seen with the previous three generations of solution seams, their occurrence between fault segments suggests that they are relatively younger than the segments themselves, i.e. younger than the three generations of solution seams described earlier. This fourth generation of solution seams controls subsequent breaching of the relay zones and linkage of fault segments to form fault zones hundreds of metres long. The example shown in Fig. 8 illustrates the common case in which segment linkage occurs by shearing along the fourth generation of solution seams. En échelon veins also occur within the relay ramps and may link, forming faults that consist of composite pull-aparts. Such faults accommodate minor amounts of antithetic slip and are sometimes sigmoidal. At the tips of these antithetic faults, tail cracks and solution seams may form in the contractional and extensional quadrants, respectively (Fig. 8). The solution seams at the tip of the antithetic faults are sub-parallel to the fourth-generation solution seams, and the relative timing of the two is uncertain. Tail cracks and solution seams sometimes occur near the tips of sheared

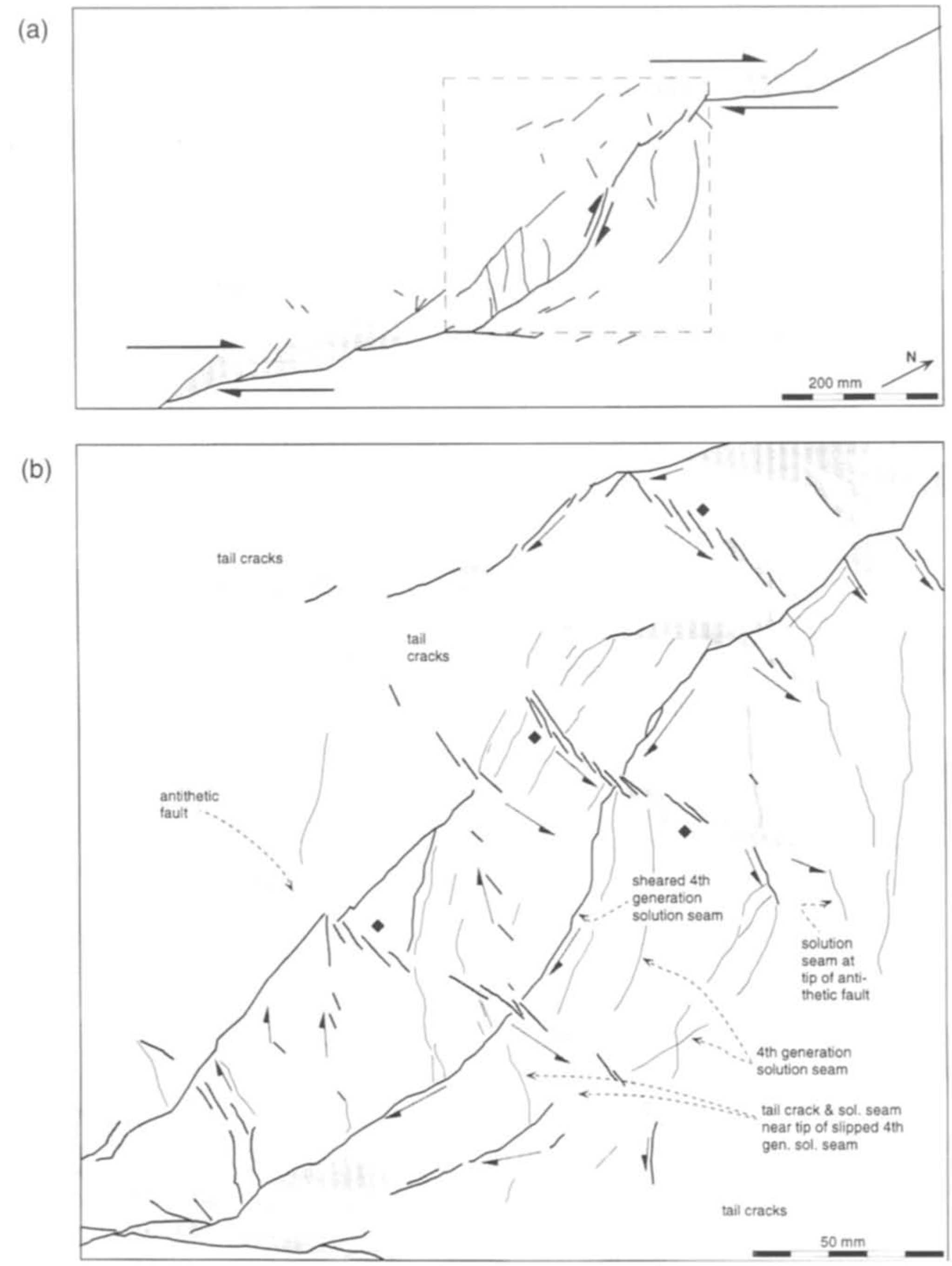

Fig. 8. A contractional strike-slip relay ramp between two overlapping fault segments (cf. Peacock and Sanderson, 1995b, fig. 1a). (a) Overview of the relay. Note pull-aparts and long thin calcite veins bounding the relay ramp. (b) Detail of the structures within the relay ramp. A high density of solution seams (thin black lines) occurs within the relay ramp. These fourth-generation solution seams are often curved and oriented obliquely to the boundary faults. Some seams have slipped to form a through-going curved slip surface that links the side-stepping segments. Early en échelon veins have linked to form minor antithetic faults, some of which are sigmoidal. Solution seams and tail cracks occur at the tips of some of these antithetic faults and near the ends of slipped fourth-generation solution seams. The diamonds indicate the locations of thin veinlets associated with some pull-aparts.

fourth-generation solution seams (lower right in Fig. 8b). These solution seams would be part of the fifth generation of solution seams. The variety of structures and geometries in m-scale relay ramps is well illustrated by Peacock and Sanderson (1995a), although their maps do not generally illustrate the solution seam patterns.

MODEL FOR FAULT DEVELOPMENT

The spatial distribution of the structures and their cross-cutting relationships can be synthesized into a two-dimensional model for temporal fault evolution in the Somerset limestone. According to this model, strike-slip

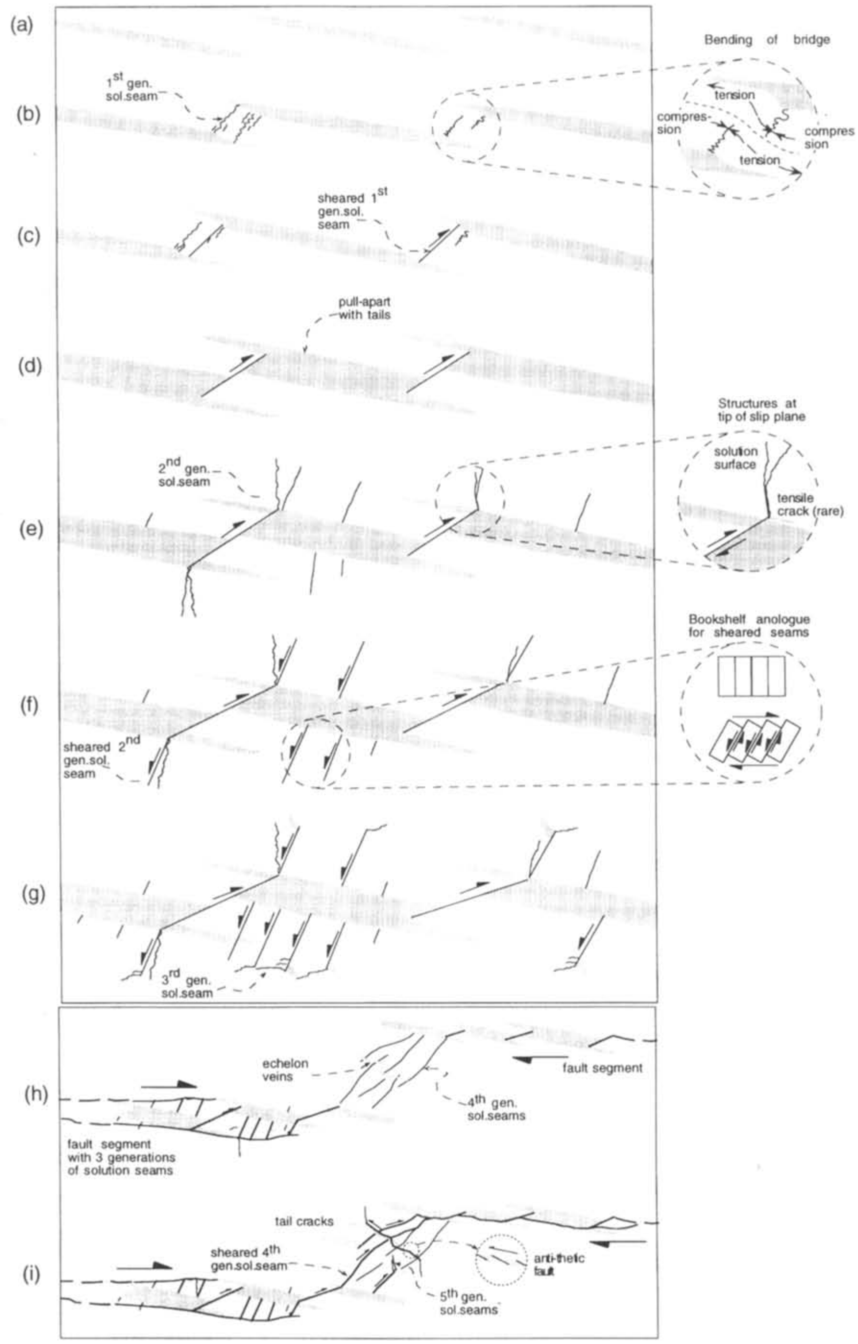

Fig. 9. Schematic model for the development of a single fault-zone segment. (a) Initial stage of en échelon veins. (b) Development of two symmetrically arranged zones of solution seams in the contractional arches of the bending bridge. (c) Incipient pull-aparts form because of shear along the solution seams. (d) Continued shear along first-generation solution seams leads to the development of pull-aparts. (e) Second generation of solution seams, as well as tail cracks, form at the tips of sheared first-generation solution surfaces. (f) Antithetic slip occurs along second-generation solution seams oriented at a high angle to the fault zone. (g) Third generation of solution seams, as well as tail cracks, form at the tips of the sheared second-generation solution seams, forming a complex anastomosing network of discontinuities across the fault zone, with block rotation occurring. (h) Solution seams and en échelon veins form in a contractional relay ramp between two side-stepping fault segments. (i) Syn- and antithetic slip along the solution seams and en échelon veins causes the formation of opening-mode tail cracks and solution seams, progressively fragmenting the relay ramp. A curved, through-going fault may develop along the fourth generation of solution seams, linking both fault segments.

faulting starts with the formation of an array of en échelon opening-mode veins (Fig. 9a). As the veins become longer and wider, they approach one another and interact. The effects of interaction are demonstrated clearly by the tapered shape of the vein in the region of overlap (Delaney and Pollard, 1981; Nicholson and Pollard, 1985; Peacock, 1991). As the veins open further, the intact rock bridge between them bends and solution seams form in the contractional arches of the bridge (Fig. 9b, see inset). With continued vein opening and shear along the vein array the bridge rotates, and one or more solution seams extend further. Eventually the solution seams are subjected to shear due to increased rotation, and start to slip (Fig. 9c). A fault zone is formed by slip along the solution seams, linking the veins and producing pull-aparts. Continued shear along the solution seams widens the pull-aparts, some of which include tails that represent ends of the original veins (Fig. 9c & d).

Gamond (1983) discussed the origin of pull-aparts with tails, and argued that veins initiate as shear fractures which open up only when they are linked by the later slip planes. As pointed out by Peacock and Sanderson (1995b), however, the occurrence of calcite-filled tails, and the direction of calcite fibres sometimes observed within the tails, suggest that the veins originate as opening-mode fractures. Their conclusion is supported by the progressive evolution from en échelon veins to pull-aparts, as shown in Figs 3–5.

There is an important difference between the model presented here and that proposed by Peacock and Sanderson (1995b), who recognized the close association of slip planes and pressure solution. They proposed that the slip planes that connect en échelon veins originated as shear fractures due to stress re-orientation in the bridges, with further stress refraction causing pressure solution on the shear fractures. Gamond (1983, 1987) and Gratier and Gamond (1990) also proposed a shear origin for the slip planes, which they called P-shears. Our observations in the bridges between overlapping veins, however, strongly suggest that these slip planes initiated as solution seams, with slip only occurring later as the bridges rotate (Fig. 4). The implication of this subtle but important difference will be discussed later.

As shear increases along the slip planes, the pull-aparts widen further and the tails may be sheared off. A second generation of solution seams forms, preferentially concentrated at the tips of the slip planes (Fig. 9e, see inset). Narrow veinlets may also form, but on the other side of the slip plane. The spatial relationship between the second generation of solution seams and the veinlets at the tip of slip planes is like that of stylolites and tail cracks observed at the tip of some strike-slip faults (Rispoli, 1981; Petit and Mattauer, 1995). The veinlets and tail cracks form in the extensional quadrant; the solution seams and stylolites in the contractional quadrant (see the inset to Fig. 6). Fletcher and Pollard (1981) show that the orientation and location of the solution seams compare favourably with the stress field around the tip of a Mode II crack. In such models, calcite-filled tail cracks are idealized as a Mode I crack with separating walls. Points on either side of a solution seam, in contrast, move towards one another as dissolved material is removed. Therefore, a solution seam can be idealized by an anti-Mode I crack for which the crack walls interpenetrate. Based on the Mode I and anti-Mode I models, Pollard and Segall (1987) and Petit and Barquins (1988) showed that the pattern of tail cracks and solution seams at the fault tip is consistent with fracture mechanics predictions and experiments, respectively.

The second-generation solution seams are orientated at a high angle to the fault zone. As slip across the zone increases further, closely spaced sets of these seams may behave as the sliding surfaces between tilting books on a bookshelf, causing antithetic slip across the second generation of solution seams (Fig. 9f, see inset). The slip associated with this block rotation leads to the formation of tail cracks and a third generation of solution seams at the tips of the sheared second-generation solution seams (Fig. 9g). At this stage, the shear displacement is several tens of millimetres and an irregular through-going break has been established. The fault zone, which has been progressively fragmented by opening-mode fracturing and pressure solution, contains numerous discontinuities with a wide variety of angles to the zone. Additional displacement can accumulate by slip along these subsidiary planes, without necessitating formation of new breaks.

Strike-slip faults hundreds of metres long, with several metres of displacement, form by the linkage of side-stepping fault segments. This process is illustrated in Fig. 9(h & i). The fourth generation of pressure-solution seams develops preferentially in the contractional relay zones between side-stepping segments. En échelon veins may also occur, forming the precursors of minor antithetic faults (Fig. 9h). Slip along the solution seams and along the minor antithetic faults can lead to the generation of other solution seams and tail cracks. In this way the relay zone becomes progressively more 'fragmented' as displacement accumulates. Linkage is achieved along a series of through-going, curved slip plane(s) that are sheared fourth-generation solution seams (Fig. 9i). Fault growth by the linkage of smaller segments has been described along other faults (e.g. Martel *et al.*, 1988; Cartwright *et al.*, 1995) but involving mechanisms other than pressure solution.

In this fault model, solution seams play a key role during the nucleation and growth of individual fault segments, and subsequently during the linkage of such segments. At least five generations of solution seams can be recognized. The distinction of different generations of solution seams is intended primarily to describe the hierarchy of structures with respect to one another and to reflect the sequence of events at one particular location on the fault zone. It is possible that the different generations of solution seam may form synchronously at different locations of a propagating fault. Solution seams of each of the various generations serve as pre-existing discontinuities along which slip can occur. In this case the prime role of pressure solution is to create potential sliding surfaces, rather than to remove irregularities or asperties on the fault plane (Marshak *et al.*, 1982).

Observations of Stockdale (1922) and Durney (1974) show that solution seams form perpendicular to the greatest compressive principal stress with no shear traction to drive slip across the seams. Two hypotheses can be presented to explain sheared solution seams. According to the first hypothesis, the fault-zone material rotates as displacement across the zone increases. Rotation of solution seams away from the principal stress plane would result in shear traction across them, allowing slip to occur. The antithetic sense of slip along the second generation of solution seams is consistent with rotation models (Nur *et al.*, 1986).

According to the second hypothesis, there is a temporal change in the stress field. Fracturing and slip may be short-lived processes, for example related to seismic events. Pressure solution, on the other hand, is a slower process, more likely to act predominantly in the inter-seismic period (Gratier and Gamond, 1990). The location of solution seams and tail cracks at fault tips and the angles between solution seams and tail cracks both suggest that these structures developed in a locally perturbed stress field (Fletcher and Pollard, 1981; Willemse and Pollard, in press). It is possible that pressure solution occurred mainly in the inter-seismic period, gradually relieving the local stress concentrations and altering the stress state with time. As the local stress perturbation decayed with time, it is possible that the solution seams were subjected to shear traction, perhaps related to the remote stress field.

Gratier and Gamond (1990) provide a detailed discussion of the role of pressure solution in crustal-scale faulting and the seismic cycle. They note that the behaviour of the fault zone depends on rock fluid content, solubility of certain rock minerals in this fluid, geometry and length-scale of the mass transfer path, value of the coefficient of mass transfer (by diffusion or infiltration), type of limiting process (reaction kinetics, mass transfer rate), stress level, temperature and confining pressure conditions. If dissolution–deposition mechanisms can accommodate the displacement rate (e.g. imposed along plate boundaries), motion along the fault is by creep. In this case slip, dissolution and precipitation can be truly contemporaneous. If accommodation by mass transfer is not sufficient, the stress level increases and an earthquake is likely to occur in the form of a periodic instability. In this case, slip, dissolution and precipitation occur in repeated cycles.

Based on the mapped structures and their cross-cutting relationships it is not possible to determine whether these faults were creeping or seismically active. The requirement that mass must be conserved suggests that the average slip rate cannot have exceeded the rate at which mass transfer can accommodate the imposed deformation. This can be achieved by balancing material sinks (material dissolved along solution seams, some of which may be slipping) against material sources (material deposited in veins and in opening pull-aparts). We believe that pressure solution, formation of pull-aparts, mineralization and the accumulation of slip are intimately related.

COMPARISON WITH OTHER STRIKE-SLIP FAULTS

Brittle failure of rock under compression has been the subject of numerous experimental studies (see Menendez *et al.*, 1996 for a recent overview). Propagation of faults in shear has been observed in sand-box and soil mechanics experiments in which unconsolidated or poorly lithified granular materials are deformed under low confining pressures (less than 5–15 MPa). In these experiments faults localize by particulate flow, i.e. the sliding, rolling and rotation of intact grains past one another (Mandl *et al.*, 1977; Borradaile, 1981; Knipe, 1989; Franssen *et al.*, 1994). At very high confining pressures, deformation is not localized on the sample scale and is thus macroscopically ductile (Wong, 1990). No distinct faults develop under such conditions, and deformation may be accommodated by crystal plasticity (dislocation glide, climb, crystal twinning, etc.) or by pervasive microcracking, also called cataclastic flow (Logan, 1987; Hirth and Tullis, 1994; Menendez *et al.*, 1996). Knipe (1989) provides a comprehensive review of the various deformation mechanisms and their relationship to strain rate, temperature, etc., and describes the microstructure characteristics of the various failure processes.

In cases other than the above, brittle faulting in experiments usually is accompanied by dilatancy and microcracking. Microcracking is observed in samples covering a variety of rocks such as granites (Peng and Johnson, 1972; Tapponier and Brace, 1976; Lockner *et al.*, 1992), sandstones (Dunn *et al.*, 1973; Menendez *et al.*, 1996) and marbles (Olsson and Peng, 1976; Fredrich *et al.*, 1989). Localized shear failure appears to be a progressive process consisting of the initiation, localization, propagation and coalescence of opening-mode microcracks. Microcracks can occur within or along the boundaries of grains or crystals. The first microcracks develop randomly within deforming samples but concentrate along a damage zone with increasing stress. Coalescence of microcracks eventually produces a surface along which macroscopic failure takes place (Borg *et al.*, 1960; Brace and Bombolakis, 1963; Scholz, 1968; Peng and Johnson, 1972; Dunn *et al.*, 1973; Engelder, 1974; Lockner *et al.*, 1992; Wong *et al.*, 1992; Zhao *et al.*, 1993). Gay and Ortlepp (1979) infer the same processes and sequence of events from observations along deep, mining-induced faults. Along ancient natural faults microfracturing is also abundant (Friedman, 1969; Engelder, 1974; Knipe and White, 1979; Kanaori *et al.*, 1991; Anders and Wiltschko, 1994). Aydin (1978) and Antonellini *et al.* (1994) document how microcracking leads to the development of cataclastic band faults that are common in some porous sandstones. Although some details remain unresolved, there is abundant evidence that brittle fault nucleation and growth occurs by slip along pre-existing discontinuities such as (coalesced) microcracks and grain boundaries (Menendez *et al.*, 1996).

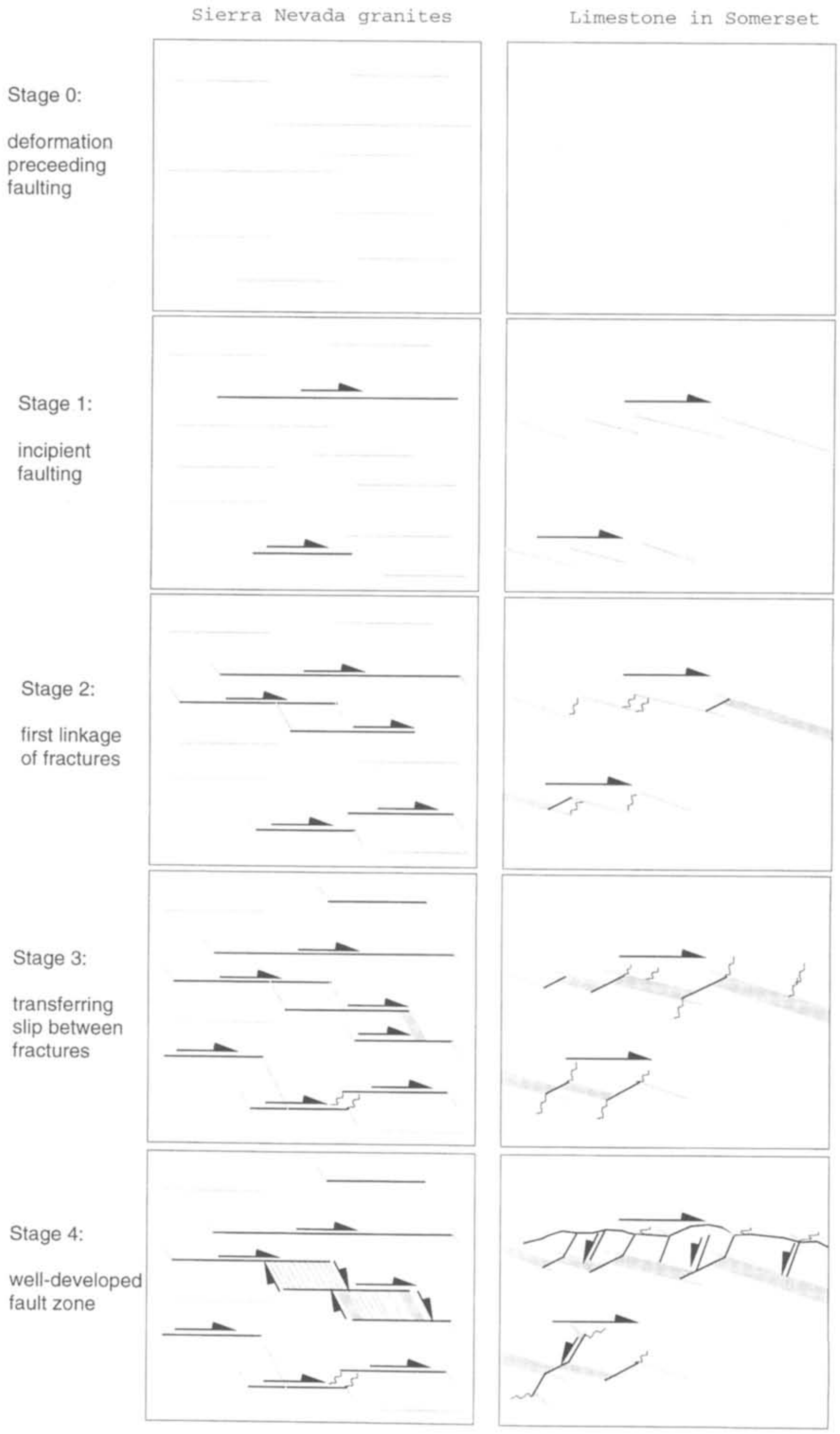

Fig. 10. Comparison between strike-slip fault models proposed for Sierra Nevada granites (Martel *et al.*, 1988) and the Somerset limestone. In the Sierra Nevada granites faulting is preceded by an earlier episode of jointing. Actual Sierra Nevada faults are left-lateral, but are drawn here as right-lateral to facilitate comparison with the other figures. See text for further discussion.

Pre-existing opening-mode cracks not only influence fault nucleation and growth at the microscopic scale, but also at the macroscopic field scale. Segall and Pollard (1983) demonstrate that strike-slip faults in the granitic rocks of the Sierra Nevada nucleated along older, mineral-filled opening-mode joints (Fig. 10, stages 0 and 1). These m-scale joints were formed during a previous deformation event, and their pattern cannot be correlated with the subsequent fault zones. The faults nucleated by slip along these pre-existing joints. Small opening-mode tail cracks propagated from near the ends of these faulted joints, at a high angle to the joint plane (Fig. 10, stage 3). The faulted joints did not propagate in shear into intact granite, but were linked by the tail cracks. The linked faulted joints are longer, and thus can accommodate more slip than individual faulted joints. Such extra slip can cause separation of tail crack walls, forming rhomb-like pull-aparts (Fig. 10, stage 3). This mechanism for pull-apart formation is different to that described earlier for the limestones. With increasing shear, pairs of small faults in the granite linked up side-to-side to form fault zones, yet the majority of slip was accommodated on the boundaries of these fault zones (Fig. 10, stage 4). Slip along fractures connecting the two boundary faults is generally synthetic, transferring slip from one boundary fault to the next. In a later paper Martel *et al.* (1988) expand this model, suggesting that the longer faults reduce the shear stresses on adjacent smaller faults, causing slip on the latter to cease. In this way, displacement is progressively localized on the longer faults. The initial phases of the same process, with sheared joints linking along tail cracks, have been observed in other granites, schists and gneisses (Granier, 1985), and in sandstones (Cruikshank *et al.*, 1991).

The limestone fault model has both similarities and differences with the experimental data and with the granite fault model. The similarity is that in all these cases, slip planes do not originate in shear; they initiate as pressure-solution seams (anti-cracks) in the Somerset limestones, and as opening-mode cracks and joints in experiments and granites. In the field, this can be noticed at a variety of scales. This observation has important fundamental applications for the micromechanics of faulting. It suggests that Mode II does not operate as a primary fracture mechanism, but only as a macroscopic phenomenon following Mode I or anti-Mode I deformation. Such a role for solution seams has not been recognized earlier, perhaps because it is difficult to study experimentally the influence of pressure solution on faulting.

In the Somerset limestones, slip occurs mainly along clay-enriched solution seams, and is rare along veins and tail cracks which are presumably stronger because of the calcite cement. It is conceivable that the concentration of clay material along the solution seams encourages slip along them, as clay gouge may reduce the shear strength (Summers and Byerlee, 1977). The principle of slip planes nucleating on pre-existing discontinuities could also explain why the dihedral angle between conjugate shear planes is often greater than 90°, at odds with Coulomb failure theory (Peacock and Sanderson, 1995a); slip along pre-existing discontinuities can occur at dihedral angles of up to 120° (Donath, 1961).

There are two interrelated differences between the limestone and granite models, illustrated schematically in Fig. 10. In the Somerset limestones incipient shear causes formation of the N–S veins that are concentrated in zones and are arranged en échelon with a consistent sense of step. Their formation is an integral part of the faulting process. In the Sierra Nevada granites, in contrast, the joints formed during an earlier event not related to subsequent faulting. In this case, the joints form a more distributed network with no systematic en échelon arrangement (stages 0 and 1, Fig. 10).

The second difference between the two fault models is that the slip planes originate as solution seams or veins, respectively. Solution seams have an opposite displacement sense to opening joints because material points on either side of a solution seam move towards one another, rather than away from one another (Fletcher and Pollard, 1981). These contrasting origins are a direct consequence of the initial joint or vein configuration. In the Somerset limestones left-stepping en échelon veins form due to right-lateral shear. For this sense of step and shear, linkage across the bridges cannot occur along tail cracks as these would be directed away from the neighbouring vein (stages 1–3, Fig. 10). The mechanisms of linkage and pull-apart shown in stage 3 of Fig. 10 are different to those observed in the Sierra Nevada granites. There is no systematic sense of step of the pre-existing joints. It is to be expected that, depending on the sense of step, faulted joints may link by tail cracks (right-stepping joints) or sheared pressure-solution seams (left-stepping joints; Fig. 10). In the Sierra Nevada granites linkage appears to occur primarily along tail cracks in extensional steps (Segall and Pollard, 1983), although contractional relays with mylonitic fabrics also occur (Bürgmann and Pollard, 1994). In other granites linkage across contractional steps involves pressure solution. P-shears that breach contractional steps between adjacent veins have been described by Gamond (1983, 1987). Gamond (1987) showed that slip along P-shears must be accompanied by local removal of material. Although Gamond argues, based on Coulomb failure theory, that these P-planes originated in shear, it is possible that they also originated as solution seams similar to those observed in the Somerset limestones.

It is likely that the model for the Somerset faults is applicable to other faults and rock types. Localization of solution seams in bridges between en échelon veins occurs in limestones in the Pyrenees (Ramsay and Huber, 1987, fig. 26.46). Pull-apart structures with tails have been reported from limestones along the Basque coast, Spain, and the Savoie, France (Robert, 1979; Gamond, 1983). Concentration of solution seams at the corners of some pull-apart structures also occurs in these areas (Gamond, 1983, fig. 1a). Rispoli (1981) and Petit and Mattauer (1995) describe sheared stylolites with tail cracks and solution seams at their tips in limestones of the Matelles outcrop, Languedoc, France. In the same outcrops a concentration of solution seams occurs in m-scale contractional relay zones between strike-slip faults (Gamond, 1987; Petit and Mattauer, 1995). Ohlmacher and Aydin (1995) show very similar structures in carbonaceous shale and siltstone of the Ordovician Sevier Shale deformed in a thrust faulting environment in the Appalachians. The micrograph in their fig. 7 shows solution-seam patterns in a mm-scale contractional relay zone that are very similar to the m-scale relay zone shown in Fig. 8. Their fig. 4 shows clusters of solution seams at the corners of pull-aparts very similar to those marked in Fig. 6. Solution associated with slip along the so-called P-shears can also be demonstrated in Mesozoic meta-greywackes and cherts in New Zealand (Spörli and Anderson, 1980).

CONCLUSIONS

Detailed study of small-scale structures on the Somerset coast suggests that pressure solution plays a key role during nucleation, growth and linkage of strike-slip fault zones in the limestones of Somerset. Pressure-solution seams serve as pre-existing discontinuities along which slip occurs during various stages of fault development during progressive deformation. There are at least five generations of solution seams, related to three different mechanisms. The first generation forms due to bending of the intact rock between overlapping opening-mode veins, with bending being indicated by the form of the bridge. As displacement along the fault zone increases, the veins link by slip along the solution seams, creating pull-aparts. A second generation of solution seams, as well as opening-mode tail cracks, form at the tips of the sliding early seams. Subsequent shear along this second generation accommodates additional fault displacement, and forms at their tips the third generation of solution seams as well as another generation of tail cracks. These first three generations all contribute to the formation of individual fault segments. The fourth and subsequent generations of solution seams form in relay zones between fault segments and control the linkage of segments, forming the next hierarchy of fault structure. Larger-scale relay zones are also fragmented by the same processes allowing adjacent fault segments to link, eventually producing a longer and wider fault zone with several metres of displacement.

In the fault zones considered here, shear is preceded or accompanied by the development of en échelon veins, tail cracks and solution seams. As fault slip accumulates, these structures form an increasingly denser network of discontinuities at various hierarchical stages. Such discontinuities occur at a variety of orientations and progressively fragment the fault-zone material at several scales. Slip occurs mostly along clay-enriched solution seams, presumably because they are weaker than calcite-filled veins.

To conserve mass, opening-mode fracturing, dissolution and slip along solution seams, mineral precipitation, and fault slip must be closely interrelated. At least two possibilities exist for the detailed temporal relationship among these processes. On the one hand, it is possible that vein opening and fault slip occur at a relatively slow rate (e.g. fault creep). If the deformation rate is slow enough compared to the rock solubility, mass transfer may fully accommodate slip accumulation, and slip, dissolution and precipitation can be truly contemporaneous. On the other hand, it is possible that fracturing and slip occur very rapidly, e.g. during seismic events, with pressure solution taking place in the longer inter-seismic period to gradually relieve the local stress perturbations. At this stage, it cannot be determined which of these possibilities is most appropriate for the faults in Somerset.

The notion that slip planes nucleate on pre-existing discontinuities is in good agreement with other field studies and with experimental data on the micromechanics of the faulting process. In experiments such pre-existing discontinuities originate as (coalesced) microcracks or grain boundaries. The field observations reported here indicate that solution seams can fulfil the same role as microcracks in localizing shear failure leading to through-going slip planes. This role for solution seams has not been recognized earlier and provides an additional micromechanical model for fault nucleation. The proposed model may be applicable to other fault zones because the characteristic structures have been described along faults in a variety of rock types. The field data lend further support to the notion that Mode II does not operate as a primary fracture mechanism, but only as a comparatively late macroscopic phenomenon that exploits pre-existing planes of weakness. In the limestones described here, the planes of weakness are formed by pressure-solution seams.

Acknowledgements—We would like to thank Ridvan Karpuz, Laurent Maerten, Dave Pollard, Keith Rawnsley and Dave Sanderson for the cordial and occasionally heated discussions on the outcrop structures that helped shape our ideas. Financial support by the Rock Fracture Project at Stanford University and by a Shell Research B.V. (The Netherlands) summer grant to E. Willemse are gratefully acknowledged. A McGee grant from the Department of Geological and Environmental Sciences covered fieldwork expenses. The Department of Geological Sciences of the University of Plymouth kindly provided transportation. We thank Mrs Dorothy Peacock for her warm hospitality, and Marie-Thérèse and Fer for support. Paula's contribution and encouragement in all those rainy days are especially acknowledged. Mark Swanson and Michael Gross provided constructive reviews.

REFERENCES

Anders, M. H. and Wiltschko, D. V. (1994) Microfracturing, paleostress and the growth of faults. *Journal of Structural Geology* **16**, 795–815.

Antonellini, M. A., Aydin, A. and Pollard, D. D. (1994) Microstructure of deformation bands in porous sandstones at Arches National Park, Utah. *Journal of Structural Geology* **16**, 941–959.

Aydin, A. (1978) Small faults formed as deformation bands in sandstone. *Pure and Applied Geophysics* **116**, 913–930.

Aydin, A. and Johnson, A. M. (1978) Development of faults as zones of deformation bands and slip surfaces in sandstone. *Pure and Applied Geophysics* **116**, 931–942.

Borg, I.Y., Friedman, M., Handin, J. and Higgs, D.V. (1960) Experimental deformation of St. Peter sand: a study of cataclastic flow. *Memoirs of the Geological Society of America* **79**, 133–191.

Borradaile, G. J. (1981) Particulate flow and the generation of cleavage. *Tectonophysics* **72**, 306–321.

Bowyer, M. O. N. and Kelly, P. G. (1995) Strain and scaling relationships of faults and veins at Kilve, Somerset. *Proceedings of the Ussher Society* **8**, 411–415.

Brace, W. F. and Bombolakis, E. G. (1963) A note on brittle crack growth in compression. *Journal of Geophysical Research* **68**, 3709–3713.

Brace, W. F., Paulding, B. W. and Scholz, C. H. (1966) Dilatancy in the fracture of crystalline rocks. *Journal of Geophysical Research* **71**, 3939–3942.

Brooks, M., Trayner, P. M. and Trimble, T. J. (1988) Mesozoic reactivation of Variscan thrusting in the Bristol Channel area, U.K. *Journal of the Geological Society of London* **145**, 439–444.

Bürgmann, R. and Pollard, D. D. (1994) Strain accommodation about strike-slip fault discontinuities in granitic rock under brittle-to-ductile conditions. *Journal of Structural Geology* **16**, 1655–1674.

Cartwright, J. A., Trudgill, B. D. and Mansfield, C. S. (1995) Fault growth by segment linkage: an explanation for scatter in maximum displacement and trace length data from the Canyonlands Grabens of SE Utah. *Journal of Structural Geology* **17**, 1319–1326.

Chadwick, R. A. (1986) Extension tectonics in the Wessex Basin, southern England. *Journal of the Geological Society of London* **143**, 444–465.

Cruikshank, K. M., Zhao, G. and Johnson, A. M. (1991) Analysis of minor fractures associated with joints and faulted joints. *Journal of Structural Geology* **13**, 865–886.

Delaney, P. T. and Pollard, D. D. (1981) Deformation of host rocks and flow of magma during growth of minette dikes and breccia-bearing intrusions near Ship Rock, New Mexico. *U.S. Geological Society Professional Paper* **1202**, 1–61.

Donath, F. A. (1961) Experimental study of shear failure in anisotropic rocks. *Bulletin of the Geological Society of America* **72**, 985–990.

Donato, J. A. (1988) Possible Variscan thrusting beneath the Somerton Anticline, Somerset. *Journal of the Geological Society of London* **145**, 431–438.

Dunn, D. E., LaFountain, L. J. and Jackson, R. E. (1973) Porosity dependence and mechanism of brittle fracture in sandstones. *Journal of Geophysical Research* **78**, 2403–2417.

Durney, D. W. (1974) The influence of stress concentrations on the lateral propagation of pressure solution zones and surfaces. *Geological Society of Australia, Tectonics and Structural Newsletter* **3**, 19.

Engelder, T. (1974) Cataclasis and the generation of fault gouge. *Bulletin of the Geological Society of America* **85**, 1515–1522.

Engelder, T. (1989) Analysis of pinnate joints in the Mount Desert Island granite: implications for post-intrusion kinematics in the coastal volcanic belt, Maine. *Geology* **17**, 564–567.

Fletcher, R. C. and Pollard, D. D. (1981) Anti-crack model for pressure solution surfaces. *Geology* **9**, 419–424.

Franssen, R. C. M. W., Peach, C. J. and Willemse, E. J. M. (1994) Fault sealing mechanisms in sandstones. In *1994 AAPG Annual Meeting, Denver*, p. 151. American Association of Petroleum Geologists.

Fredrich, J. T., Evans, B. and Wong, T. F. (1989) Micromechanics of the brittle to plastic transition in Carrara Marble. *Journal of Geophysical Research* **94**, 4129–4145.

Friedman, M. (1969) Structural analysis of fractures in cores from the Saticy field, Ventura Co, California. *Bulletin of the American Association of Petroleum Geologists* **53**, 367–389.

Gamond, J. F. (1983) Displacement features associated with fault zones: a comparison between observed examples and experimental models. *Journal of Structural Geology* **5**, 33–45.

Gamond, J. F. (1987) Bridge structures as sense of displacement criteria in brittle fault zones. *Journal of Structural Geology* **9**, 609–620.

Gay, N. C. and Ortlepp, W. D. (1979) Anatomy of a mining-induced fault zone. *Bulletin of the Geological Society of America* **90**, 47–58.

Granier, T. (1985) Origin, damping, and pattern of development of faults in granite. *Tectonics* **4**, 721–737.

Gratier, J. P. and Gamond, J. F. (1990) Transition between seismic and aseismic deformation in the upper crust. In *Deformation Mechanisms, Rheology and Tectonics*, eds R. J. Knipe and E. H. Rutter, pp. 461–473. Geological Society of London Special Publication **54**.

Hancock, P. L. (1985) Brittle microtectonics: principles and practice. *Journal of Structural Geology* **7**, 269–276.

Hancock, P. L. and Barka, A. A. (1987) Kinematic indicators on active normal faults in western Turkey. *Journal of Structural Geology* **9**, 573–584.

Hirth, G. and Tullis, J. (1994) The brittle–plastic transition in experimentally deformed quartz aggregates. *Journal of Geophysical Research* **99**, 11731–11748.

Horsfield, W. T. (1977) An experimental approach to basement controlled faulting. *Geologie en Mijnbouw* **56**, 363–370.

Kanaori, Y., Yairi, K. and Ishida, T. (1991) Grain boundary microcracking of granitic rocks from the northeastern region of the Atotsugawa fault, central Japan: SEM backscattered electron images. *Engineering Geology* **30**, 221–235.

Knipe, R. J. (1989) Deformation mechanisms: recognition from natural tectonites. *Journal of Structural Geology* **11**, 127–146.

Knipe, R. J. and White, S. H. (1979) Deformation in low grade shear zones in Old Red Sandstone, S.W. Wales. *Journal of Structural Geology* **1**, 53–66.

Lockner, D. A., Byerlee, J. D., Kuksenko, V., Ponomarev, A. and Sidorin, A. (1992) Observations of quasistatic fault growth from acoustic emissions. In *Fault Mechanics and Transport Properties of Rock*, eds B. Evans and T.-F. Wong, pp. 1–31. Academic Press, San Diego.

Logan, J. M. (1987) Porosity and the brittle–ductile transition in sedimentary rocks. *AIP Conference Proceedings* **154**, 229–242.

Maltman, A. J. (1987) Shear zones in argillaceous sediments; and experimental study. In *Deformation of Sediments and Sedimentary Rocks*, eds M. E. Jones and M. F. Preston, pp. 77–87. Geological Society of London Special Publication **29**.

Maltman, A. J. (1994) Prelithification deformation. In *Continental Deformation*, ed. P. L. Hancock, pp. 143–158. Pergamon, New York.

Mandl, G., de Jong, L. N. J. and Maltha, A. (1977) Shear zones in granular material. *Rock Mechanics* **9**, 95–144.

Marshak, S., Geiser, P. A., Alvarez, W. and Engelder, T. (1982) Mesoscopic fault array of the northern Umbrian Apennine fold belt, Italy: Geometry of conjugate shear by pressure solution slip. *Bulletin of the Geological Society of America* **93**, 1013–1022.

Martel, S. J., Pollard, D. D. and Segall, P. (1988) Development of simple strike-slip fault zones, Mount Abbot quadrangle, Sierra Nevada, California. *Bulletin of the Geological Society of America* **100**, 1451–1465.

McCoss, A. M. (1986) Simple constructions for deformation in transpression/transtension zones. *Journal of Structural Geology* **8**, 715–718.

McLachlan, A. C. (1986) A revised interpretation of the structures within the Mesozoic of north-west Somerset. M.Sc. thesis, Imperial College, London.

Menendez, B., Zhu, W. and Wong, T. F. (1996) Micromechanics of brittle faulting and cataclastic flow in Berea sandstone. *Journal of Structural Geology* **18**, 1–16.

Moore, D. E. and Lockner, D. A. (1995) The role of microcracking in shear-fracture propagation in granite. *Journal of Structural Geology* **17**, 95–114.

Nicholson, R. and Pollard, D. D. (1985) Dilation and linkage of en échelon cracks. *Journal of Structural Geology* **7**, 583–590.

Nur, A., Ron, H. and Scotti, O. (1986) Fault mechanics and the kinematics of the block rotations. *Geology* **14**, 746–749.

Ohlmacher, G. C. and Aydin, A. (1995) Progressive deformation and fracture patterns during foreland thrusting in the southern Appalachians. *American Journal of Science* **295**, 943–987.

Olsson, W. A. and Peng, S. S. (1976) Microcrack nucleation in marble. *International Journal of Rock Mechanics and Mining Science, and Geomechanics Abstracts* **13**, 53–59.

Peacock, D. C. P. (1991) A comparison between the displacement geometries of veins and normal faults at Kilve, Somerset. *Proceedings of the Ussher Society* **7**, 363–367.

Peacock, D. C. P. and Sanderson, D. J. (1991) Displacements, segment linkage and relay ramps in normal fault zones. *Journal of Structural Geology* **13**, 721–733.

Peacock, D. C. P. and Sanderson, D. J. (1992) Effects of layering and anisotropy on fault geometry. *Journal of the Geological Society of London* **149**, 793–802.

Peacock, D. C. P. and Sanderson, D. J. (1995) Pull-aparts, shear fractures and pressure solution. *Tectonophysics* **241**, 1–13.

Peacock, D. C. P. and Sanderson, D. J. (1995) Strike-slip relay ramps. *Journal of Structural Geology* **17**, 1351–1360.

Peacock, D. C. P. and Zhang, X. (1994) Field examples and numerical modelling of oversteps and bends along normal faults in cross section. *Tectonophysics* **234**, 147–167.

Peng, S. and Johnson, A. M. (1972) Crack growth and faulting in cylindrical specimens of Chelfsford granite. *International Journal of Rock Mechanics and Mining Science, and Geomechanics Abstracts* **9**, 37–86.

Petit, J. P. and Barquins, M. (1988) Can natural faults propagate under mode-II conditions? *Tectonics* **7**, 1243–1256.

Petit, J. P. and Mattauer, M. (1995) Palaeostress superimposition deduced from mesoscale structures in limestone: the Matelles exposure, Lanquedoc, France. *Journal of Structural Geology* **17**, 245–256.

Pollard, D. D. and Segall, P. (1987) Theoretical displacements and stresses near fractures in rock: with applications to faults, joints, veins, dikes, and solution surfaces. In *Fracture Mechanics of Rocks*, ed. B. K. Atkinson. Academic Press Geology Series. Academic Press, London.

Price, N. J. and Cosgrove, J. W. (1990) *Analysis of Geological Structures*. Cambridge University Press, Cambridge.

Ramsay, J. G. and Huber, M. I. (1987) *Modern Structural Geology, Volume 2: Folds and Fractures*. Academic Press, London.

Rispoli, R. (1981) Stress fields about strike-slip faults inferred from stylolites and tension gashes. *Tectonophysics* **75**, T29–T36.

Robert, I. (1979) Etude des mecanismes de plissement d'une série stratifiée dans une zone de cisaillement: exemple de la côte Basque. These 3eme cycle thesis, Grenoble.

Rudnicki, J. W. and Rice, J. R. (1975) Conditions for the localization of deformation in pressure sensitive dilatant materials. *Journal of Mechanics, Physics and Solids* **23**, 371–394.

Scholz, C. H. (1968) Microfracturing and inelastic deformation of rock in compression. *Journal of Geophysical Research* **73**, 1414–1432.

Segall, P. and Pollard, D. D. (1983) Nucleation and growth of strike slip faults in granite. *Journal of Geophysical Research* **88**, 555–568.

Spörli, K. B. and Anderson, H. J. (1980) Paleostress axes from mineral striations in faulted Mesozoic basement, Auckland, New Zealand. *New Zealand Journal of Geology and Geophysics* **23**, 155–166.

Stockdale, P. B. (1922) *Stylolites; Their Nature and Origin*. Indiana University Studies **9**, 1–97.

Summers, R. and Byerlee, J. (1977) A note on the effect of fault gouge composition on the stability of frictional sliding. *International Journal of Rock Mechanics and Mining Science* **14**, 155–160.

Tapponier, P. and Brace, W. F. (1976) Development of stress induced microcracks in Westerly granite. *International Journal of Rock Mechanics and Mining Science, and Geomechanics Abstracts* **13**, 103–112.

Whittaker, A. G. G. W. (1983) Geology of the Country Around Weston-super-Mare, sheet 279 and parts of sheets 263 and 295. *Memoirs of the Geological Survey of Great Britain*.

Willemse, E. J. M. and Pollard, D. D. (in press) On the orientations and patterns of wing cracks and solution seams near the tip of a sliding flaw or fault. *Journal of Geophysical Research*.

Wong, T.-F. (1990) Mechanical compaction and the brittle–ductile transition in porous sandstones. In *Deformation Mechanisms, Rheology and Tectonics*, eds R. J. Knipe and E. H. Rutter, pp. 111–122. Geological Society of London Special Publication **54**.

Wong, T.-F., Szeto, H. and Zhang, J. (1992) Effect of loading path and porosity on the failure mode of porous rocks. *Applied Mechanics Reviews* **45**, 281–293.

Zhao, Y., Huang, J. and Wang, R. (1993) Real-time SEM observations of the microfracturing process in rock during a compression test. *International Journal of Rock Mechanics and Mining Science, and Geomechanics Abstracts* **30**, 643–652.